Variations and predictability of epistasis on an intragenic fitness landscape.

Sarvesh Baheti[1], Namratha Raj[2], Supreet Saini[2,*]

[1] Department of Chemical Engineering, Indian Institute of Technology Jodhpur, India

[2] Department of Chemical Engineering, Indian Institute of Technology Bombay, India

* Corresponding author. Email: saini@che.iitb.ac.in, Phone: +91 22 2576 7216

Abstract

How epistasis hinders or facilitates movements on fitness landscapes has been a longstanding question of interest. Several high throughput experiments have demonstrated that despite its idiosyncrasy, epistatic effects exhibit global statistical patterns, namely, diminishing returns and increasing costs. Recently, Papkou et. al. constructed a fitness landscape for a 9-base region in the *folA* gene, which encodes for Dihydrofolate Reductase (DHFR), in *E. coli*, and demonstrated that despite being highly rugged, the landscape is highly navigable. In this work, using the *folA* landscape data we ask two questions: (1) How does the nature of epistatic interactions change as a function of the genomic background? (2) How predictable is epistasis within a gene? We show that mutations exhibit one of two binary "states": a small fraction of mutations exhibit extremely strong patterns of global epistasis, while most do not. As against this binary classification, epistasis is also very "fluid" - the nature of epistasis exhibited by a pair of mutations is strongly contingent on the genetic background. Despite this strong dependency, we observe that the DFE of a genotype is highly predictable based on its fitness. These results offer a perspective on how epistasis operates within a gene, and how it can be predicted.

Keywords: *epistasis, fitness landscapes, folA, diminishing returns, increasing costs*

Introduction

Despite their geometric simplicity, fitness landscapes have invited contrasting views ever since their proposal (1). While Wright proposed that the ruggedness of landscapes implied that non-adaptive forces were needed for a population's increase in fitness, Fisher argued that the high dimensionality of real landscapes implied that natural selection was sufficient to ensure continuous adaptation.

In recent years, several attempts, ranging from a few mutations to several thousand, have been made to characterize fitness landscapes empirically (2). Most of these attempts have focused on a handful of "important" sites in a protein, and some mutations in these sites have been mapped with macroscopic fitness traits such as growth rate (3-9). Results from these studies show that idiosyncratic epistasis leads to rugged fitness landscapes of proteins, indicating that protein evolution is constrained (10, 11), although epistasis can facilitate evolution of novel functions too (12). Fitness landscapes are also constructed by considering mutations across the genome (13, 14). All these studies indicate the adaptation is unpredictable.

On the other hand, data from laboratory evolution experiments show that evolutionary processes follow certain statistical rules. Fitness effect of a mutation decreases with increase in background fitness (diminishing returns epistasis) (15, 16), the deleterious effect of a mutation increases with increase in background fitness (increasing costs epistasis) (14), and that the availability of beneficial mutations decreases with increase in background fitness (17). Studies from a number of organisms and in a variety of environmental contexts have demonstrated that these basic principles of evolution are universal (14, 15, 18-23). Such qualitative statistical convergence makes evolution qualitatively predictable.

Clearly, there are two contradicting views of the predictability of epistasis.

In a recent study, Papkou et al constructed a landscape of a 9-base pair sub-sequence of the *folA* gene in *Escherichia coli* (*E. coli*) (24). The landscape was multipeaked with 514 fitness peaks, indicating a rugged landscape. Papkou and coworkers show that despite the ruggedness, the highest peaks in the landscape were surprisingly easily accessible.

In this work, we analyze the landscape presented by Papkou and coworkers (24), to test Fisher's hypothesis and our current understanding of evolutionary constraints. As the landscapes' size increases, fewer sites have access to the highest peak – contrary to Fisher's proposal. Our work shows that the nature of epistasis between two mutations is highly fluid, and contingent on the genetic background. However, the DFE of a genotype is predictable solely by fitness which is a

macroscopic trait, and is independent of the specific genotype. This makes predicting evolution possible with information about a trait as macroscopic as growth rate.

Results

Frequency of fitness peaks decreases with size of the landscape.

The number of peaks increases exponentially, as a function of sequence length (**Figure 1A**). We create subgraphs from a 9-base landscape, so subgraphs of the same size differ in numbers of peaks, resulting in a distribution for each *n*-base pair landscape ($\boldsymbol{n} < 9$). The mean, median statistics of the peaks of these landscapes for each value of *n* is shown. Papkou and coworkers group all sequences into two – "functional" and "non-functional". However, their groupings are statistical and not functional, and hence, we call them high and low fitness genotypes. While in Figure 1A, we only show data for sequences corresponding to high fitness, including all sequences in the analysis does not change this result qualitatively (**Supplement Figure S1**).

We use a maximally rugged (uncorrelated) NK-landscape model to predict the expected number of peaks in a *n*-base pair landscape. Our results show that while the median number of peaks in the landscape distribution is a good predictor of the number of peaks, a large number of landscapes, for any size *n*, do not follow the predicted NK peak distributions (**Figure 1** and **Supplement Figure S2**).

As *n* increases, while the size of the landscape and the number of peaks both increase exponentially, although the increase in the number of peaks is much slower. Hence, the probability of any given point being a peak decreases with increasing *n* (**Figure 1B**). Our results also show that as the size of the landscape increases, the variation between different subgraphs of the same size decreases, and makes structure of landscapes statistically predictable.

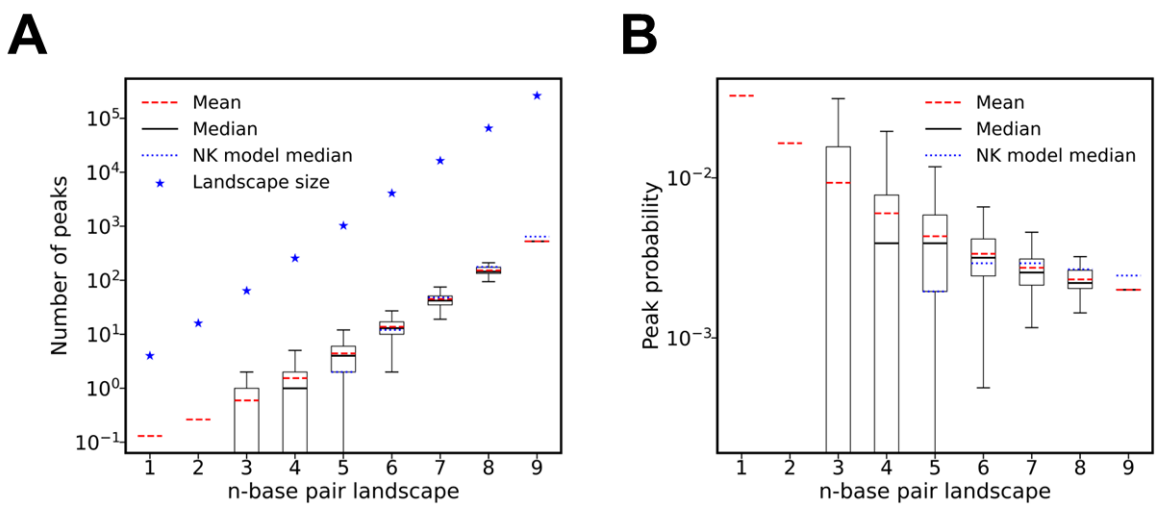

Figure 1. Probability of peaks in landscapes decreases with size. (A) The number of high fitness peaks increase exponentially as we increase the size of the landscape, albeit at a slower rate than the increase of size of landscape. **(B)** The probability of a randomly picked point being a high fitness peak decreases with increase in the size of the landscape.

Mutations on the landscape exhibit diminishing returns and increasing costs.

Fitness effect of a mutation is contingent on the genetic background (25, 26). These effects often manifest as diminishing returns and increasing costs. We analyze the effect of mutations in the landscape, and quantify the fitness effect of the mutation as a function of the fitness of the background on which it occurs. All high fitness backgrounds were analyzed for effects of all single nucleotide mutations on them (**Figure 2A**). These high fitness backgrounds, collectively, exhibit diminishing returns for beneficial mutations and increasing costs for deleterious mutations. These statistical relations, however, are weak (R^2 = 0.1284).

Backgrounds with lower fitness exhibit a different trend. In what are characterized as "non-functional" variants in the study by Papkou et. al., a single peaked distribution is seen for a given background fitness, with a weak global epistasis linear fit (**Figure 2B**) (R^2 = 0.1236). As the background fitness increases, high- and low-fitness backgrounds exhibit decreasing mean of the DFE (**Figure 2C-D).**

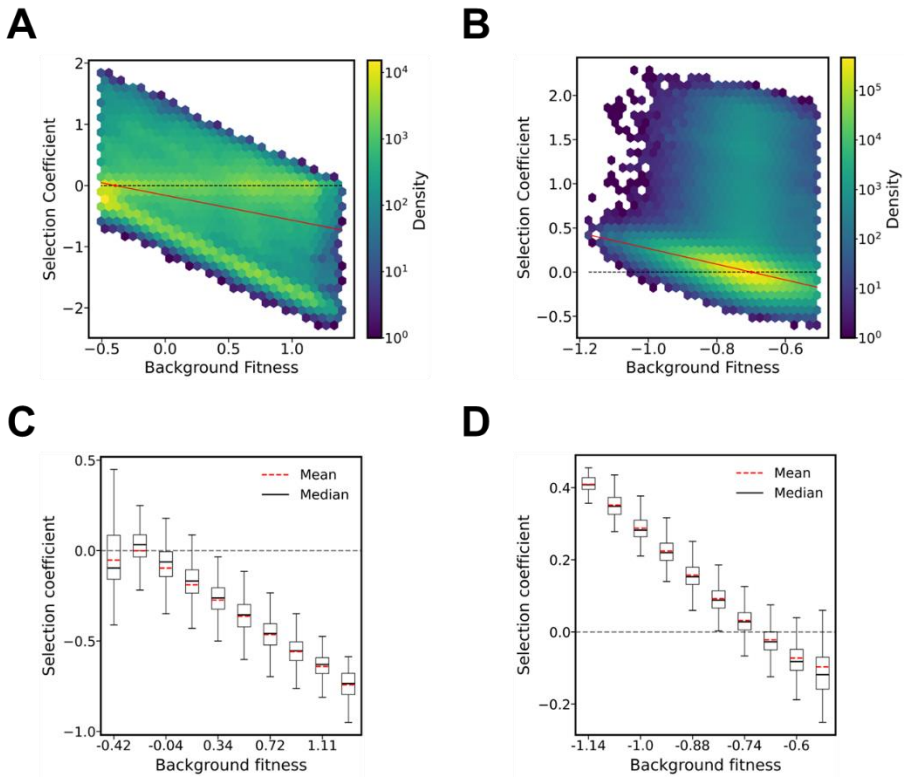

Figure 2. (A) Mutational effects vs. the background fitness for all high fitness sequences show a two peaked global epistatic pattern (R^2 0.1284). **(B)** The diminishing return pattern for sequences with low fitness is much weaker, and single peaked (R^2 0.1236). Mean fitness of DFE decreases with background fitness for **(C)** high fitness backgrounds and **(D)** low fitness backgrounds.

In Figure 2, we show effect of all mutations in high fitness (Figure 2A) and low fitness (Figure 2B) backgrounds. We next investigate the effect of each of the 108 (12 possible mutations at each of the 9 sites) mutations in the *folA* landscape individually, and test their impact in different backgrounds. **Figure 3** shows that only a few mutations exhibit very strong patterns of global epistasis. An overwhelming majority of mutations exhibit no correlation ($R^2 < 0.2$) between their fitness effect and the fitness of the background on which they occur (**Supplement Figure S3**).

A recent report (27) studying patterns of “microscopic” epistasis in yeast reports a “pivot” growth rate. The “pivot” growth rate is the growth rate at which any mutation switches from being beneficial (when background fitness is below the “pivot”) to deleterious (when background fitness is above the “pivot”). This phenomenon likely represents deep fundamental “rule” of how a cell works. We test the existence of the pivot growth rate for each of the 108 mutations in the *folA* sequence. More than 90% mutations “pivot” from being beneficial to deleterious at a growth rate -0.657 ± 0.065 (**Figure 4**). The occurance of a “pivot” growth rate despite poor statistical correlations between background fitness and effect of a mutation is a surprising observation.

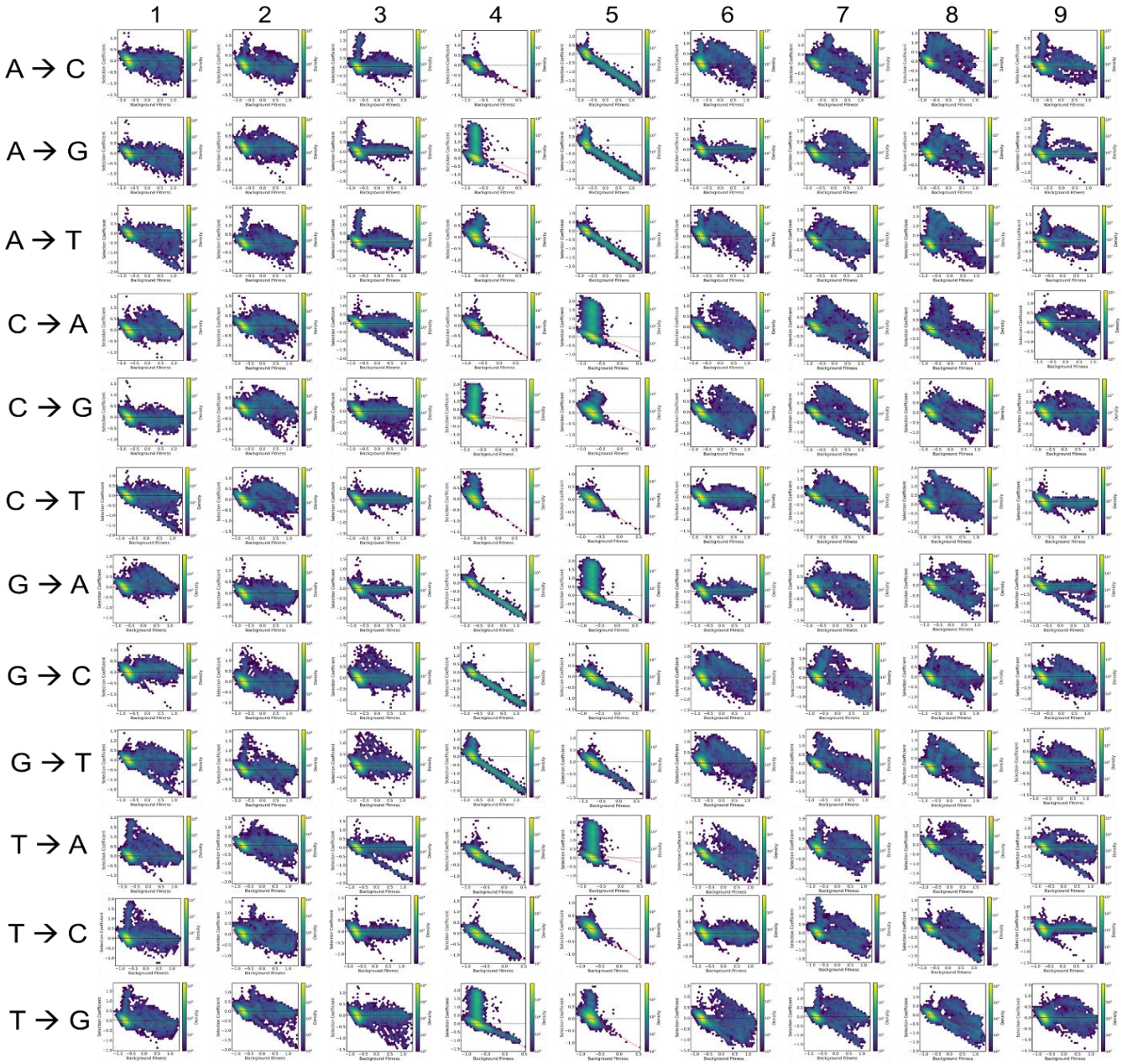

Figure 3. Only a small fraction of mutations exhibits patterns of global epistasis. Only 14 (all at position 4 and 5) out of 108 mutations exhibit statistically significant patterns ($R^2 > 0.4$) of global epistasis. See **Supplement Table 1** for detailed statistics for each mutation.

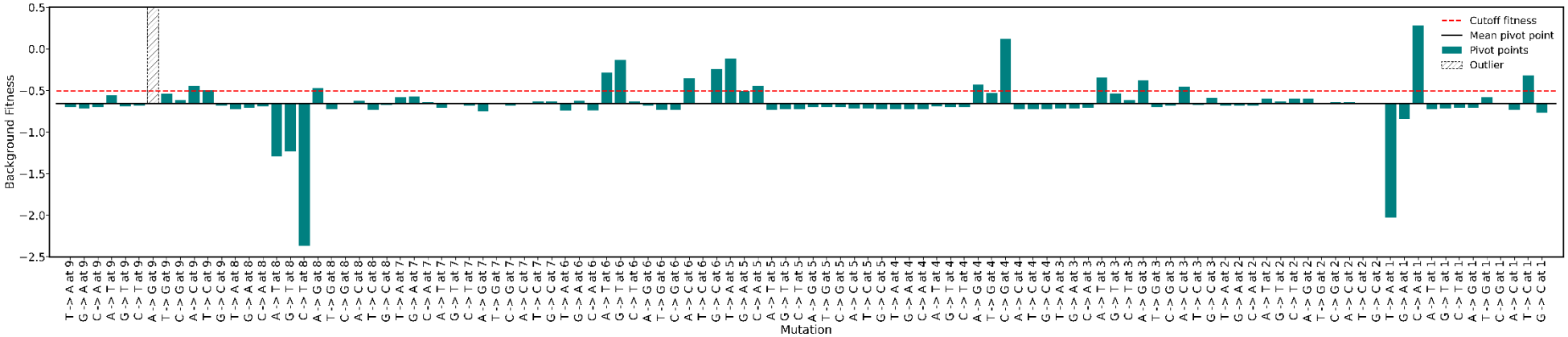

Figure 4. Background fitness (y-axis) at which each of the 108 mutations switches from beneficial to deleterious. The black solid line shows the average fitness at which the nature of the mutation pivots. Bars show the deviation from the average for each mutation. 90% of the mutations exhibit the “pivot” growth rate within 10% of each other. This mean pivot growth rate is indicated by the black solid line (background fitness -0.657). The dotted line in red indicates the growth rate used in Papkou et al (24) to differentiate between high and low fitness variants.

DFE of a mutant can be successfully predicted from the "phenotypic DFE".

Of the ~4^9 genotypes in the landscape, several exhibit near identical fitness. We binned all genotypes in non-overlapping fitness intervals of 0.05, and the collective DFE of all genotypes in a bin was computed. We term this distribution as the "phenotypic DFE" of the genotypes exhibiting nearly identical fitness. DFE of high fitness backgrounds comprised of two peaks: the first peak corresponds to mutations with large deleterious effects, while the second peak (centered at selection coefficient, $s \sim 0$) corresponds to mutations which are nearly neutral (**Figures 5A**). For low fitness variants, the DFE comprised of only one peak, centered at roughly $s \sim 0$ (**Figure 5B**). Both, the fraction of mutations which are beneficial, and the mean quantum of benefit conferred by a beneficial mutation decrease with increasing fitness.

We next ask how robustly can the DFE of a particular genotype be predicted solely from the "phenotypic DFE", as shown in Figure 5A. To test this, we sampled up to 100000 pairs of different focal variant sequences within each non-overlapping interval of 0.05 background fitness, and examined the DFE for each genotype sampled. The Mann-Whitney U test performed on all sampled background pairs indicated that the DFE of any sequence can be statistically predicted from the "phenotypic DFE" (**Figure 5C**). The prediction improved as the background fitness of the genotypes increased.

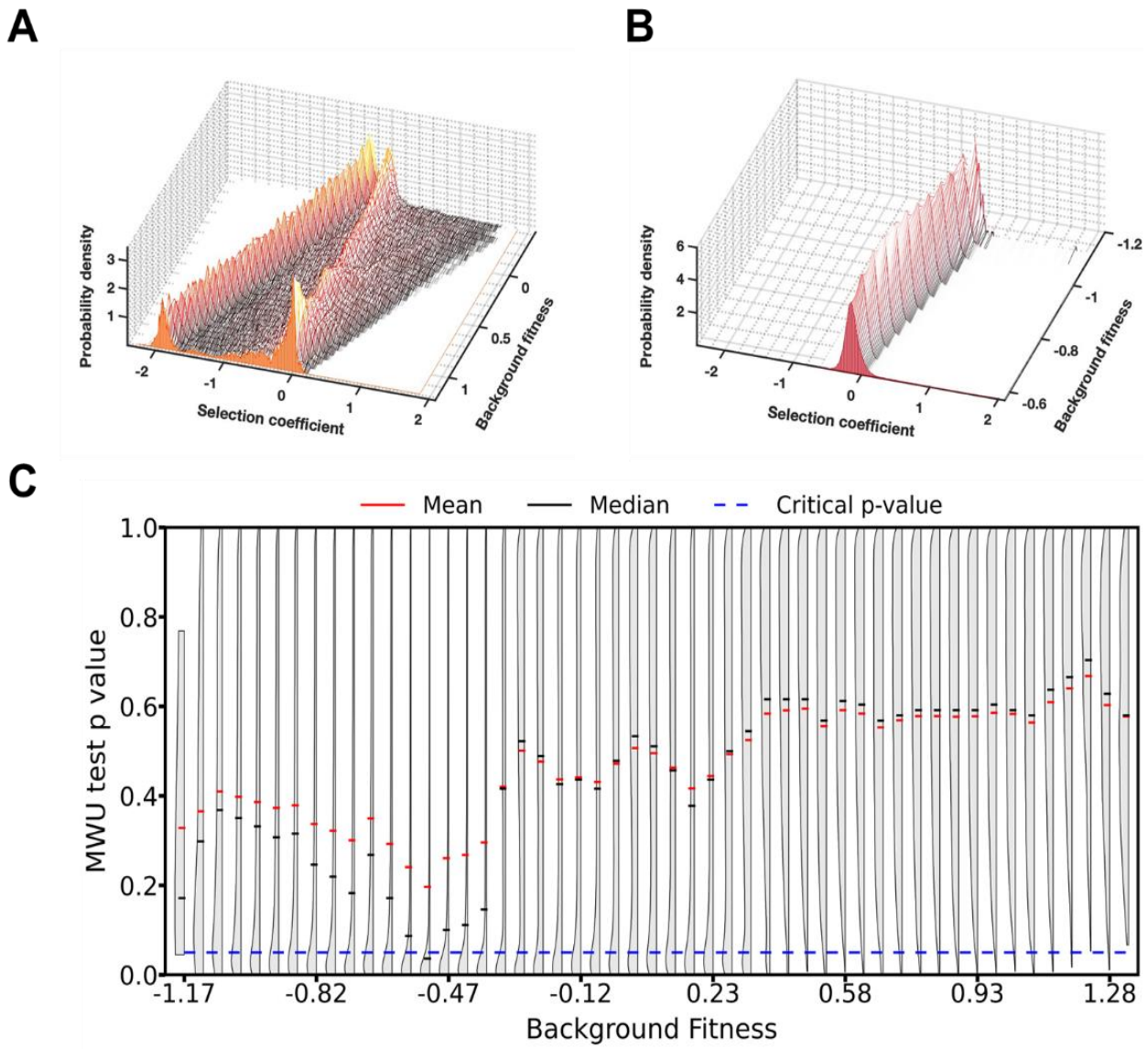

Figure 5. The "phenotypic DFE" of *folA*. (A) Distribution of fitness effects (probability distribution of selection coefficient) of all high fitness backgrounds at different background fitness are overlapped (on x-axis) to form the structure of the phenotypic DFE. The DFE qualitatively remains the same for all high fitness variants: the first peak (from left; at s≈-2) in the DFE signify "lethal" mutations which contribute in making the variant low fitness (hence, as the background fitness increases, we observe the peak move to left). The second peak in the DFE, situated at s=0 signify a large fraction of "neutral" mutations. Additionally, as the background fitness increases, the extent of benefit conferred by beneficial mutations diminishes, as predicted from diminishing returns epistasis. **(B)** Distribution of fitness effects of low fitness backgrounds. Qualitatively, the fitness effects of low fitness backgrounds show a gaussian distribution with minimal spread, highlighting the unlikelihood of a low fitness variant achieving functionality equivalent to a high fitness background due to a single mutation. **(C)** Distribution of p-values from a MWU-test to determine statistical similarity between the DFEs of variants with similar fitness, In each band of 0.05 fitness, up to 100000 genotypes pairs were sampled and their statistical similarity was tested to create the distribution of p-values. The high p-value for all variants as we move far from the cutoff fitness (-0.508) show high p-value, validating the hypothesis that the individual DFEs of variants with very similar fitness are sampled from the same parent distribution. Since all these tested variants compose the "phenotypic DFE", we can conclude that all individual high fitness DFEs are indeed sampled from the "phenotypic DFE".

Nature of epistasis between two mutations is context dependent.

Epistasis is pervasive and idiosyncratic, and between two mutations, *A* and *B*, can manifest as no, positive, negative, or sign epistasis. While epistasis' effect on protein evolution, adaptation has been investigated deeply, we do not know how fluid the nature of epistatic interactions is. We ask how the nature of epistatic interactions between *A* and *B* changes as a function of the genomic background. How frequent (or rare) is this phenomenon (where nature of epistasis changes), and are there changes in nature of epistasis (say, positive to sign) which are more frequent than other transitions? In other words, we seek epistatic interactions between a locus *X* and loci *A* & *B*, which change the nature of epistasis between *A* and *B* (**Figure 6A**).

To answer this question, we analyzed the combined effect of all 576 mutation pairs ($\binom{9}{2}4^2$) in the 9-base pair *folA* sequences. For our study, we classified epistasis into six categories: Positive epistasis (PE), Negative epistasis (NE), No epistasis (No) and sign epistasis was further classified into Reciprocal Sign epistasis (RSE), Single Sign epistasis (SSE) and Other Sign epistasis (OSE) based on the number of paths restricted to Darwinian evolution (**see methods**). The frequency of the different epistatic interactions vary with the functionality of the genotype. In high fitness backgrounds, mutation pairs exhibit positive epistasis most frequently (median 39%), followed by negative epistasis (median 27%) and no epistasis (median 20%), with sign epistasis being relatively rare (**Figure 6B**).

In low fitness backgrounds, mutation pairs exhibit no epistasis most frequently (median 30%), followed by negative epistasis (median 22%), positive epistasis (median 21%) and other sign epistasis (median 13%) (**Figure 6C**). We note that the variability of the nature of epistasis among mutations in high fitness backgrounds is significantly greater, as compared to the variability in the low fitness backgrounds. Thus, statistical patterns observed close to, and far from fitness peaks in the landscape are qualitatively different. Since the *folA* landscape is dominated by low fitness variants (93% of all variants), the epistatic interactions of mutations considering all variants in the landscape exhibit very similar result as the low fitness *folA* variants (**Supplementary Figure S4**).

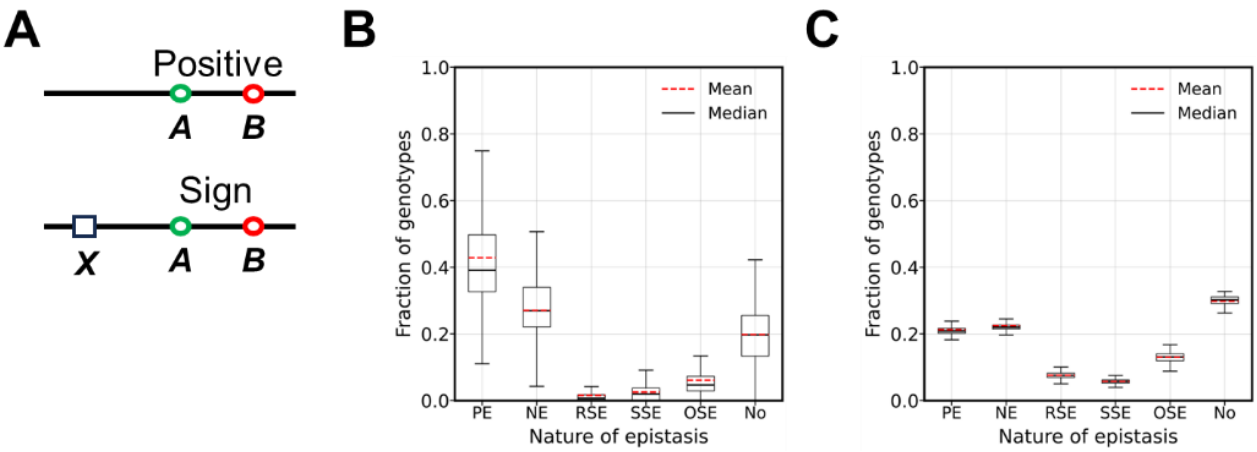

Figure 6. (A) Imagine two mutations A and B which exhibit positive epistasis. In this work, we seek existence of a mutation at another locus X, such that the nature of epistasis between A and B changes from positive epistasis to another kind (for example, sign epistasis, as shown in the Figure). **(B)** Each mutation pair in the entire set of $\binom{9}{2}$ *loci* x (4 *bases*)^2 = 576 possible mutation pairs were examined on all valid genotypes. The fraction of epistasis exhibited by each mutation pair on high fitness backgrounds was used to create the box plot. The frequency of positive epistasis is the greatest, followed by negative, and no epistasis. The frequency of the three kinds of sign-epistasis (reciprocal, single, and other) is relatively fewer. Different mutation pairs show large variance in epistatic interactions. **(C)** Epistasis observed for each mutation pair on low fitness backgrounds were used to create the box plot. The variation of frequency of different types of epistasis is much smaller and hence the nature of epistasis exhibited in low fitness variants is relatively more predictable.

Next, for a mutation pair m_1 at locus l_1 and m_2 at locus l_2 showing an epistatic interaction on a genotypic sequence $\mathcal{S}$, we quantified the number of cases where any single point mutation on $\mathcal{S}$ at a locus l_3 (other than at locus l_1 or l_2) changes the nature of epistasis exhibited between m_1 and m_2. For each mutation pair, we introduce all possible 21 single nucleotide variations (three mutations at each of the remaining seven positions in the sequence). For each sequence pair, we note if/how the nature of epistasis changes in the 21 cases examined.

The nature of epistasis in mutant sequences was dependent on the background epistasis for high fitness backgrounds (**Figure 7**). For instance, upon introduction of a third mutation, two mutations exhibiting positive epistasis were still most likely to continue to exhibit positive epistasis. However, overall, an epistatic interaction was more likely to switch to another form of epistasis, than continue to exhibit the same, upon introduction of a single mutation.

For low fitness backgrounds, upon introduction of a mutation, the nature of epistasis preferentially switched to positive, negative, or no epistasis. Sign epistasis manifested relatively infrequently, irrespective of the original nature of epistasis between m_1 and m_2 (**Figure 8**). These results again highlight the difference in the statistical behavior of landscapes in regions close to or far from fitness peaks.

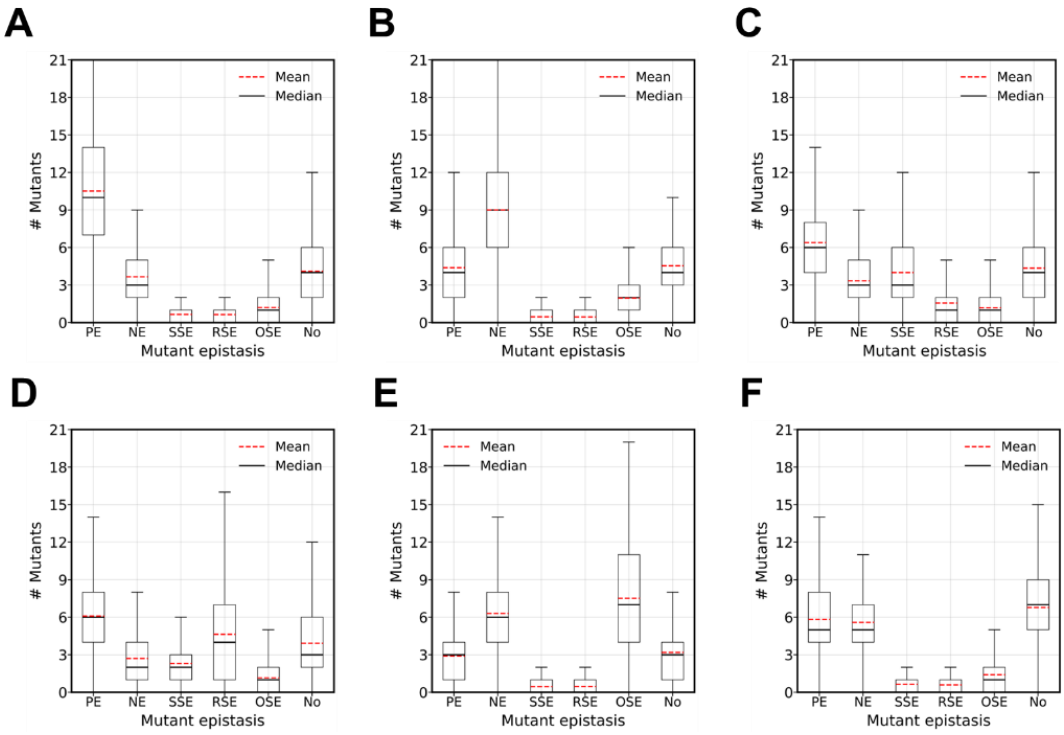

Figure 7. Change in nature of epistasis is frequent in high fitness backgrounds. Y-axis denotes the number of mutations (out of a total of 21 (7 sites x 3 possible mutations) which exhibit epistasis as indicated on the x-axis. The starting genotype had **(A)** Positive epistasis, **(B)** Negative epistasis, **(C)** Single sign epistasis, **(D)** Reciprocal sign epistasis, **(E)** Other size epistasis, and **(F)** No epistasis.

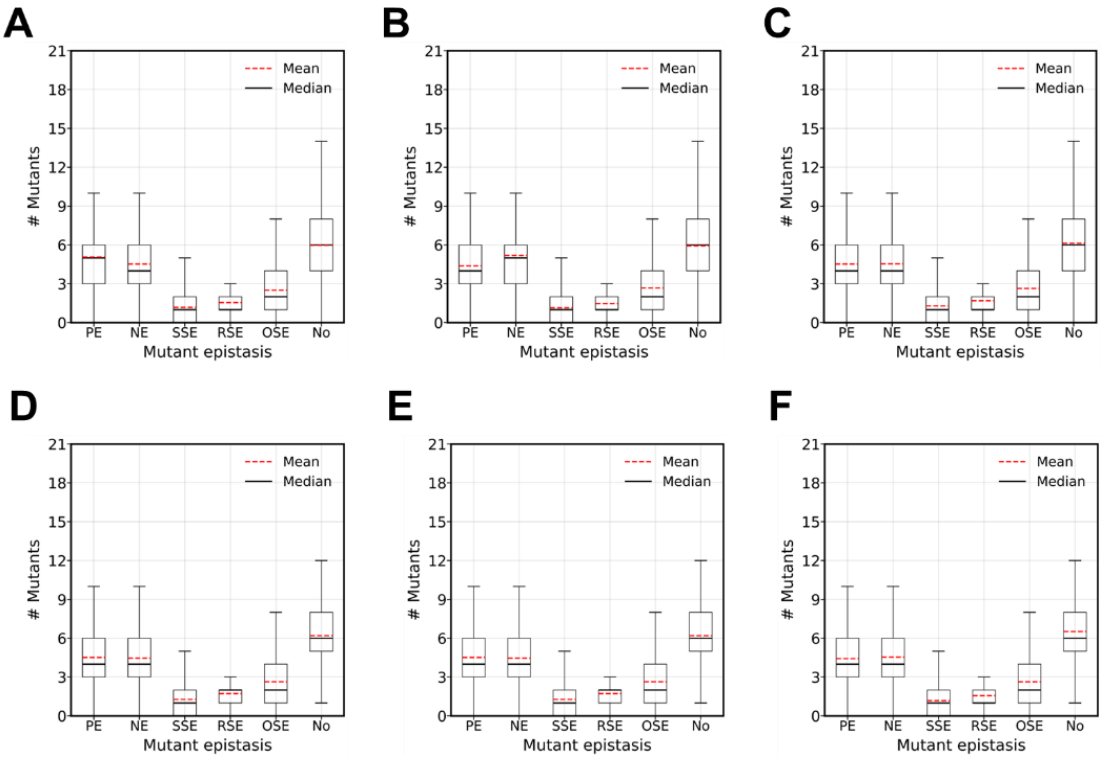

Figure 8. Change in nature of epistasis is frequent in low fitness backgrounds. Y-axis denotes the number of mutations (out of a total of 21 (7 sites x 3 possible mutations) which exhibit epistasis as indicated on the x-axis. The starting genotype had **(A)** Positive epistasis, **(B)** Negative epistasis, **(C)** Single sign epistasis, **(D)** Reciprocal sign epistasis, **(E)** Other size epistasis, and **(F)** No epistasis.

The pervasiveness of the change in epistatic interactions is surprising, and makes determination of evolutionary trajectories unpredictable. However, we also note that change of nature of epistasis due to a mutation is not unique to *folA*. An analysis of a previously published five-point landscape of beta-lactamase gene shows that change in nature of epistasis in common in intramolecular landscapes (**Supplement Figure S5**).

Accessibility to fitness peak decreases with increasing size of landscape.

The study by Papkou et al computed that 76.5% of low-fitness variants had access to high-fitness peaks, making the rugged landscape navigable. Theoretically, as we move *n* bases away from a peak on the fitness landscape, the number of shortest trajectories to the peak increases factorially (as *n!*). Though 76.5% of the variants reach peaks through random walks, the accessibility of the peak through all shortest paths is not known.

To explore this, we assessed the accessibility of the highest peak on the landscape for all variants at *n* Hamming distance. The fraction of variants which could not access the peak via even a single shortest path increased from 15% for *n* = 4, to 21% for *n* = 7 (**Figure 9**). These results demonstrate that with increasing dimensionality of the landscape, sign-epistasis poses an increasing constraint for Darwinian movement on a landscape.

In addition, the peak accessibility of variants at 2 hamming distance from the highest fitness peak in the *folA* landscape suggests that while the fraction of variants which exhibit no sign epistasis (magnitude epistasis) remain the same for low and high fitness backgrounds, the fraction of variants exhibiting reciprocal sign epistasis (no accessible paths to the highest peak) is much greater in high fitness backgrounds than in low fitness backgrounds (**Supplementary Figure S6**).

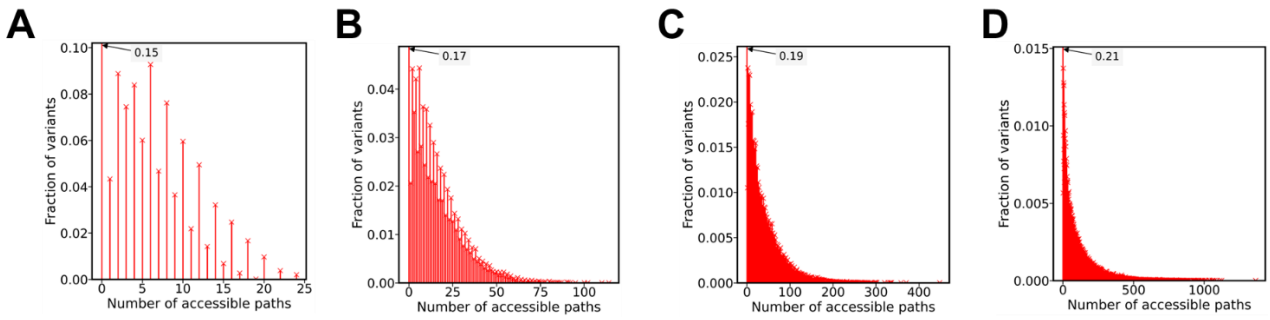

Figure 9. Path accessibility distribution to highest fitness peak for Hamming distance (A) 4, (B) 5, (C) 6, and (D) 7. As the Hamming distance increases (A to D), the fraction of points with no adaptive paths to the global peak increases from 0.15 to 0.21.

There are no evolvability enhancing mutations in *folA* landscape.

Protein evolution is known to be facilitated via evolvability enhancing mutations. Mechanistically, these mutations enhance evolution via increasing stability, or providing avenues to parts of landscape otherwise not available. However, the generality of availability of evolvability enhancing mutations is unknown.

To find out if a neutral mutation on a genotype can affect the protein evolvability, we compiled a list of all neutral mutations (with selection coefficient < 0.02). If the selection coefficient of another mutation before and after acting of this neutral mutation was s_1 and s_2, the change in selection coefficient due to this neutral mutation is $\Delta = s_2 - s_1$. Hence, we find the relative increase in selection coefficient as $r = \frac{\Delta}{|s_1|}$.

The relative increase in selection coefficient gives us an idea of the increase in evolvability of the genotype. We found that for any given neutral mutation on high fitness backgrounds, the net increase in evolvability was around zero, with notable exceptions of mutations on the highly volatile loci 4 and 5. Low fitness backgrounds, even though with high variance showed no global change in evolvability for any particular neutral mutation (**Figure 10**). Thus, in the context of *folA* landscape, no evolvability enhancing mutations exist in the nine base pair sequence.

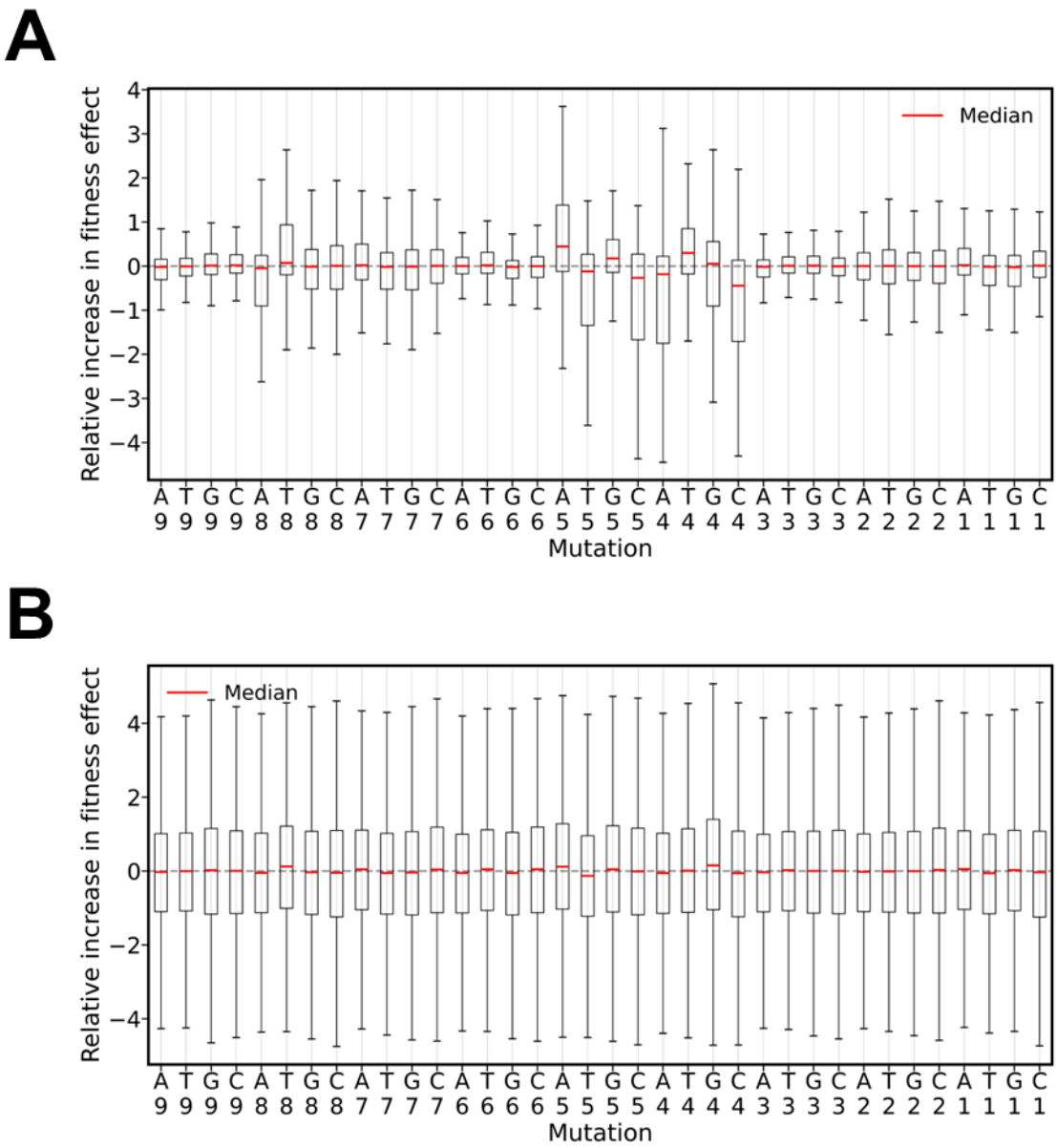

Figure 10. In the *folA* landscape, no evolvability enhancing mutations exist. X-axis represents neutral mutations (nucleotide and position), and y-axis represents the relative ratio of change in fitness pre- and post- the mutation indicated on x-axis. **(A)** For high fitness backgrounds and **(B)** for low fitness backgrounds.

Discussion

Chance and determinism dictate evolutionary trajectories. On fitness landscapes, features of mutations and adaptation such as global epistasis make evolution statistically predictable. However, epistasis, especially within a gene, can also be idiosyncratic, which makes adaptive paths unpredictable. These facets of evolutionary dynamics have been the focus of several experimental studies. In this work, we report two novel aspects of the role of epistasis in adaptation.

While epistasis makes prediction of evolutionary trajectories entrenched in complexity, the question of how fluid the nature of epistasis is between two specific mutations has remained unanswered. Our results show that the nature of epistasis between two mutations in a sequence has an extremely malleable character. Depending on the genomic background, two mutations can exhibit sign, positive, negative, or no epistasis. In fact, there is a greater than 50% chance that the nature of epistasis between two mutations changes, upon the introduction of a third mutation in the background.

While this makes the process of evolution more confounding, it also offers a mechanistic explanation of how populations can escape from local maxima on a landscape. Imagine sign epistasis between mutations *A* and *B* traps a population in a local maximum. Explaining movement out of this local maxima was, for Sewall Wright, the central problem of evolution (28). He proposed the need to invoke forces other than natural selection to ensure movement of the population out of this maximum (for Wright, this was *Shifting Balance Theory*). However, in absence of evidence in support of Wright's proposal, "*it seems unreasonable to consider the shifting balance process as an important explanation for the evolution of adaptations*" (29).

Alternatively, imagine a population stuck in a local maximum (because of sign-epistasis). Should an effectively neutral mutation change the nature of epistasis from sign- to positive (or negative) epistasis, the population is no longer confined to a local maximum, and can escape via the action of selection. Darwinian evolution is sufficient to explain movement on the landscape, albeit not via a mechanism suggested by Fisher (30). Although such potentiating mutations have been observed in laboratory evolution experiments, deciphering their adaptive effects has not been trivial (31-33). However, neutral (34) or even deleterious (35) potentiating mutations have been observed in two separate contexts.

Effects of such potentiating mutations is also known to transition from neutral to deleterious, indicating role of epistasis (33). But, our understanding of epistasis, and how it impacts adaptation are largely explained statistically (27, 36, 37), while models explaining mechanistic origins are

relatively rare (38). In the absence of any mechanistic models, which explain epistasis and its manifestations, the fluid nature of epistasis adds another layer of complexity to the prediction of adaptation and evolution.

However, the concept of “phenotypic DFE” implies that for a given genotype, we have statistically accurate predictions of its DFE. This makes tracking evolutionary trajectories easier.

A reason why fitness landscapes may indicate unpredictability in evolution is because they are constructed by considering a handful of sites, and are therefore not representative of what happens in real cells, or what real landscapes look like. Therefore, as experimentally challenging as their construction may be, high dimensional landscapes are necessary to be able to make informed comments on the fundamental constraints of adaptation.

Methods

Calculating Hamming Distance.

To calculate the hamming distance between two sequences of equal length, we compare the sequences and count the number of dissimilar loci.

Construction of sequence spaces and landscapes.

In order to construct an n-base pair sequence space from a parent p-base pair sequence space ($p > n$), we choose any $p - n$ loci in the parent sequence space and find all variants in the parent space in which the selected loci are fixed (these loci contain a same sequence). The set of these selected variants are assigned their one hamming distance neighbours to construct a new $n\text{-}base$ sequence space.
By repeating this process over all $\binom{p}{p-n}$ combinations of selecting the loci to be fixed and the 4^{p-n} permutations of choosing the fixed sequence in each case, we are able to break the parent sequence space into $\left[\binom{p}{p-n} \times 4^{p-n}\right]$ n-base pair sequence spaces (**Supplement Table 2**).

For our study, we use a nine-base pair parent sequence space to generate n-base pair sequence spaces $(1 \leq n \leq 9)$. Landscapes are generated by mapping fitness values of each sequence in a sequence space corresponding to the ones assigned in the empirical fitness landscape generated by Papkou et al. using a nine base pair gene.

In rare cases where fitness value was not known, we disregarded those variants in all studies.

Finding peaks in a fitness landscape.

<u>Number of Peaks in Landscape</u>: To count the number of peaks in fitness landscapes, we find the number of variants that have a higher fitness value than all its one hamming distance neighbours in that landscape.

<u>Peak Probability</u>: To quantify the probability of encountering a fitness peak in any landscape, we find the ratio of number of peaks found to the total number of sequences in that fitness landscape.

Expected number of peaks: In our case (as we are dealing with 4 letter genome), the expected number of peaks in maximally rugged (uncorrelated) NK landscapes is found by $\left(\frac{number\ of\ functional\ variants}{3n+1}\right)$ for an n-base pair landscape (39). The number of peaks predicted by NK landscapes is rounded off to nearest integer.

Fitness effect of mutations.

To find the fitness effect of a mutation acting on a genotype, we start with a set of all genotypes in the empirical Papkou et al. fitness landscape which would result in a new sequence formed following the mutation. In all such genotypes, we find the background fitness f_b and the fitness of resulting mutant f_m. The selection coefficient of this mutation in this background is determined as the fitness difference between the mutant and the background ($s = f_m - f_b$).

Finding phenotypic DFE: We found the Distribution of Fitness Effects for variants lying in a small slice of fitness value (for our study, we kept the range of this slice to be 0.05). The DFE was constructed by analysing the frequency of fitness effects of all mutations acting on the backgrounds lying in the selected range.

Finding genotypic DFE: For any 9 length genotypic sequence, we found the $9 loci \times 3 bases = 27$ mutations that may result in a new sequence. We used the frequency of fitness effect of all these mutations to constitute the distribution of fitness effects for any genotype.

Non parametric tests: We found the p-value of the two parameter KS test and the Mann–Whitney *U* test using the *python scipy.stats* library.

Linear regression: We found the pivot point fitness of individual mutations via linear regression of background fitness and the selection coefficient of the mutation using the “LinearRegression” model from python sklearn.linear_model library.

Epistasis as function of genetic background.

Classifying Epistasis: To quantify the epistasis present in a mutation pair acting on two differing genetic loci, we compute the fitness effect of the individual mutations on a genetic background and the cumulative fitness effect of the two mutations on the same genetic background. If the fitness effect of the individual mutations were s_1 and s_2, while the cumulative effect of the two mutations was s_{12}, then we classify the epistasis into following categories,

1. No Epistasis: If $|s_{12} - (s_1 + s_2)| < 0.05$ i.e. we assume no epistasis was present if the cumulative fitness effect of the two mutations was about the same as the two mutations acting independently on the genetic background.

2. Sign Epistasis: If $s_{12} \times (s_1 + s_2) < 0$ i.e. we classify sign epistasis if the cumulative effect of the two mutations lead to a different sign of fitness effect than the sum of individual fitness effects of the two mutations on the same background. For example, if the combined effect of the mutation pair was beneficial even though the sum of fitness effects of the two mutations on the same background was deleterious, and vice versa.

3. We further classified this epistasis into three categories,
   A. Reciprocal Sign Epistasis: If $s_1 < 0$, $s_2 < 0$ and $s_{12} > 0$ i.e. if the cumulative effect of the two mutations lead the background to a higher fitness, but both shortest paths to this higher fitness point are blocked to darwinian evolution.
   B. Single Sign Epistasis: If exclusively $s_1 < 0$ or $s_2 < 0$ and $s_{12} > 0$ i.e. if exactly one of the two shortest paths leading background to higher fitness are blocked to darwinian evolution.
   C. Other Sign Epistasis: All other cases cases classified to sign epistasis.

4. Positive Epistasis: If $s_{12} > s_1 + s_2$ i.e. if the combined fitness effect of the two mutations was more beneficial / less deleterious than the sum of individual effects of the mutation pair on the genetic background.

5. Negative Epistasis: If $s_{12} < s_1 + s_2$ i.e. if the combined fitness effect of the two mutations was less beneficial / more deleterious than the sum of individual effects of the mutation pair on the genetic background.

Epistasis Change with Genetic Background: Having the epistasis dossier generated for all mutation pairs, we compiled all cases of *Positive, Negative, Sign* and *No Epistasis*. For each of these cases, we select the genetic backgrounds and their one mutant neighbours such that their differing mutation locus is unrelated to the loci involved in Epistasis (In our case, we can find $(9 - 2) loci \times 3 bases = 21$ such neighbours for each background).

We then check the nature of epistasis in each of these 21 neighbours on the same mutation pair, and quantify the number of these cases in which nature of epistasis changes.

Finding paths in a sequence space.

Set of all variants: We start by listing all the mutations required to convert the starting sequence $A$to the target sequence T. If h denotes the minimum number of mutations required to change sequence A to T, then for each step $s \in \{1, \cdots, h-1\}$, we list all variants in the sequence space which are at s hamming distance from the starting variant and $h-s$ hamming distance from the target sequence. The resulting set includes all variants involved at each step for shortest traversal from A to T.

Having the set of all variants at each step in traversal of sequence A to T, we recursively find all $h!$ permutations of paths such that each step only allows one base change while leading the sequence to the target in minimum number of steps.

Effect of neutral mutations on evolvability.

To perform this study, we compiled all the $(9 loci \times 4 bases) = 36 mutations$ that are possible among all sequences of *folA* landscape. We then listed all the backgrounds on which these mutations change the genotype, but showcase neutral fitness effect (magnitude of selection coefficient< 0.05).

We then allow a second mutation which changes both the background and the mutant genotype. If the selection coefficient of the second mutation on the background is s_1 and on the neutral mutant is s_2, then the relative increase in evolvability is quantified as: $\left(\frac{s_2 - s_1}{|s_1|}\right)$.

Consider a variant A and a neutral mutation X which results in a variant B $(A \neq B | s_{AB}| < 0.05)$. For any mutation Y taking place on genotypes A and B forming A' and B' such that $(A \neq A' B \neq B')$, we quantify the relative change in evolvability of A from mutation Y due to a neutral mutation X as $\left(\frac{s_{BB'} - s_{AA'}}{|s_{AA'}|}\right)$.

Codes.

All codes used in this work are at https://github.com/SainiSupreet/DHFR-landscape. See **Supplement Table S3** for details.

Acknowledgements.

This work was funded by a DBT/Wellcome Trust (India Alliance) grant (award no. IA/S/19/2/504632) to SS. NMR was funded by Prime Minister's Research Fellowship (PMRF ID 1301163).

References

1. Provine WB. The Origins of Theoretical Population Genetics: The University of Chicago Press; 2001.
2. de Visser JA, Krug J. Empirical fitness landscapes and the predictability of evolution. Nat Rev Genet. 2014;15(7):480-90.
3. Hietpas R, Roscoe B, Jiang L, Bolon DN. Fitness analyses of all possible point mutations for regions of genes in yeast. Nat Protoc. 2012;7(7):1382-96.
4. Chen JZ, Fowler DM, Tokuriki N. Environmental selection and epistasis in an empirical phenotype-environment-fitness landscape. Nat Ecol Evol. 2022;6(4):427-38.
5. Karageorgi M, Groen SC, Sumbul F, Pelaez JN, Verster KI, Aguilar JM, et al. Genome editing retraces the evolution of toxin resistance in the monarch butterfly. Nature. 2019;574(7778):409-12.
6. Weinreich DM, Delaney NF, Depristo MA, Hartl DL. Darwinian evolution can follow only very few mutational paths to fitter proteins. Science. 2006;312(5770):111-4.
7. Pokusaeva VO, Usmanova DR, Putintseva EV, Espinar L, Sarkisyan KS, Mishin AS, et al. An experimental assay of the interactions of amino acids from orthologous sequences shaping a complex fitness landscape. PLoS Genet. 2019;15(4):e1008079.
8. Li C, Qian W, Maclean CJ, Zhang J. The fitness landscape of a tRNA gene. Science. 2016;352(6287):837-40.
9. Cote-Hammarlof PA, Fragata I, Flynn J, Mavor D, Zeldovich KB, Bank C, et al. The Adaptive Potential of the Middle Domain of Yeast Hsp90. Mol Biol Evol. 2021;38(2):368-79.
10. Bakerlee CW, Nguyen Ba AN, Shulgina Y, Rojas Echenique JI, Desai MM. Idiosyncratic epistasis leads to global fitness-correlated trends. Science. 2022;376(6593):630-5.
11. Starr TN, Thornton JW. Epistasis in protein evolution. Protein Sci. 2016;25(7):1204-18.
12. Metzger BPH, Park Y, Starr TN, Thornton JW. Epistasis facilitates functional evolution in an ancient transcription factor. Elife. 2024;12.
13. Fowler DM, Fields S. Deep mutational scanning: a new style of protein science. Nat Methods. 2014;11(8):801-7.
14. Johnson MS, Martsul A, Kryazhimskiy S, Desai MM. Higher-fitness yeast genotypes are less robust to deleterious mutations. Science. 2019;366(6464):490-3.
15. Chou HH, Chiu HC, Delaney NF, Segre D, Marx CJ. Diminishing returns epistasis among beneficial mutations decelerates adaptation. Science. 2011;332(6034):1190-2.
16. Kryazhimskiy S, Rice DP, Jerison ER, Desai MM. Microbial evolution. Global epistasis makes adaptation predictable despite sequence-level stochasticity. Science. 2014;344(6191):1519-22.
17. Brajesh RG, Dutta D, Saini S. Distribution of fitness effects of mutations obtained from a simple genetic regulatory network model. Sci Rep. 2019;9(1):9842.
18. Wei X, Zhang J. Patterns and Mechanisms of Diminishing Returns from Beneficial Mutations. Mol Biol Evol. 2019;36(5):1008-21.
19. Wunsche A, Dinh DM, Satterwhite RS, Arenas CD, Stoebel DM, Cooper TF. Diminishing-returns epistasis decreases adaptability along an evolutionary trajectory. Nat Ecol Evol. 2017;1(4):61.
20. Johnson MS, Desai MM. Mutational robustness changes during long-term adaptation in laboratory budding yeast populations. Elife. 2022;11.

21. Couce A, Limdi A, Magnan M, Owen SV, Herren CM, Lenski RE, et al. Changing fitness effects of mutations through long-term bacterial evolution. Science. 2024;383(6681):eadd1417.
22. Ascensao JA, Wetmore KM, Good BH, Arkin AP, Hallatschek O. Quantifying the local adaptive landscape of a nascent bacterial community. Nat Commun. 2023;14(1):248.
23. Johnson MS, Reddy G, Desai MM. Epistasis and evolution: recent advances and an outlook for prediction. BMC Biol. 2023;21(1):120.
24. Papkou A, Garcia-Pastor L, Escudero JA, Wagner A. A rugged yet easily navigable fitness landscape. Science. 2023;382(6673):eadh3860.
25. Wang Y, Arenas CD, Stoebel DM, Cooper TF. Genetic background affects epistatic interactions between two beneficial mutations. Biol Lett. 2013;9(1):20120328.
26. Chandler CH, Chari S, Dworkin I. Does your gene need a background check? How genetic background impacts the analysis of mutations, genes, and evolution. Trends Genet. 2013;29(6):358-66.
27. Ardell S, Martsul A, Johnson MS, Kryazhimskiy S. Environment-independent distribution of mutational effects emerges from microscopic epistasis. bioRxiv. 2024.
28. Wade MJ, Goodnight CJ. Wright's shifting balance theory: an experimental study. Science. 1991;253(5023):1015-8.
29. Coyne JA, Barton NH, Turelli M. Perspective: A Critique of Sewall Wright's Shifting Balance Theory of Evolution. Evolution. 1997;51(3):643-71.
30. Robert A. Skipper J. Revisiting the Fisher-Wright Controversy. Transactions of the American Philosophical Society. 2009;99:299-322.
31. Blount ZD, Borland CZ, Lenski RE. Historical contingency and the evolution of a key innovation in an experimental population of Escherichia coli. Proc Natl Acad Sci U S A. 2008;105(23):7899-906.
32. Blount ZD. A case study in evolutionary contingency. Stud Hist Philos Biol Biomed Sci. 2016;58:82-92.
33. Quandt EM, Gollihar J, Blount ZD, Ellington AD, Georgiou G, Barrick JE. Fine-tuning citrate synthase flux potentiates and refines metabolic innovation in the Lenski evolution experiment. Elife. 2015;4.
34. Despres PC, Dube AK, Grenier J, Picard ME, Shi R, Landry CR. Compensatory mutations potentiate constructive neutral evolution by gene duplication. bioRxiv. 2024.
35. Douglas SM, Chubiz LM, Harcombe WR, Marx CJ. Identification of the potentiating mutations and synergistic epistasis that enabled the evolution of inter-species cooperation. PLoS One. 2017;12(5):e0174345.
36. Reddy G, Desai MM. Global epistasis emerges from a generic model of a complex trait. Elife. 2021;10.
37. Lyons DM, Zou Z, Xu H, Zhang J. Idiosyncratic epistasis creates universals in mutational effects and evolutionary trajectories. Nat Ecol Evol. 2020;4(12):1685-93.
38. Frohlich C, Bunzel HA, Buda K, Mulholland AJ, van der Kamp MW, Johnsen PJ, et al. Epistasis arises from shifting the rate-limiting step during enzyme evolution of a beta-lactamase. Nat Catal. 2024;7(5):499-509.
39. Kauffman S, Levin S. Towards a general theory of adaptive walks on rugged landscapes. J Theor Biol. 1987;128(1):11-45.